




Rapid Growth of Uropathogenic *Escherichia coli* during Human Urinary Tract Infection

Valerie S. Forsyth,^a  Chelsie E. Armbruster,^{a*} Sara N. Smith,^a Ali Pirani,^{a,b} A. Cody Springman,^{a†} Matthew S. Walters,^{a*} Greta R. Nielubowicz,^{a*} Stephanie D. Himpf,^a Evan S. Snitkin,^{a,b} Harry L. T. Mobley^a

^aDepartment of Microbiology and Immunology, University of Michigan Medical School, Ann Arbor, Michigan, USA

^bDepartment of Internal Medicine Division of Infectious Diseases, and Center for Microbial Systems, University of Michigan Medical School, Ann Arbor, Michigan, USA

ABSTRACT Uropathogenic *Escherichia coli* (UPEC) strains cause most uncomplicated urinary tract infections (UTIs). These strains are a subgroup of extraintestinal pathogenic *E. coli* (ExPEC) strains that infect extraintestinal sites, including urinary tract, meninges, bloodstream, lungs, and surgical sites. Here, we hypothesize that UPEC isolates adapt to and grow more rapidly within the urinary tract than other *E. coli* isolates and survive in that niche. To date, there has not been a reliable method available to measure their growth rate *in vivo*. Here we used two methods: segregation of nonreplicating plasmid pGTR902, and peak-to-trough ratio (PTR), a sequencing-based method that enumerates bacterial chromosomal replication forks present during cell division. In the murine model of UTI, UPEC strain growth was robust *in vivo*, matching or exceeding *in vitro* growth rates and only slowing after reaching high CFU counts at 24 and 30 h postinoculation (hpi). In contrast, asymptomatic bacteriuria (ABU) strains tended to maintain high growth rates *in vivo* at 6, 24, and 30 hpi, and population densities did not increase, suggesting that host responses or elimination limited population growth. Fecal strains displayed moderate growth rates at 6 hpi but did not survive to later times. By PTR, *E. coli* in urine of human patients with UTIs displayed extraordinarily rapid growth during active infection, with a mean doubling time of 22.4 min. Thus, in addition to traditional virulence determinants, including adhesins, toxins, iron acquisition, and motility, very high growth rates *in vivo* and resistance to the innate immune response appear to be critical phenotypes of UPEC strains.

IMPORTANCE Uropathogenic *Escherichia coli* (UPEC) strains cause most urinary tract infections in otherwise healthy women. While we understand numerous virulence factors are utilized by *E. coli* to colonize and persist within the urinary tract, these properties are inconsequential unless bacteria can divide rapidly and survive the host immune response. To determine the contribution of growth rate to successful colonization and persistence, we employed two methods: one involving the segregation of a nonreplicating plasmid in bacteria as they divide and the peak-to-trough ratio, a sequencing-based method that enumerates chromosomal replication forks present during cell division. We found that UPEC strains divide extraordinarily rapidly during human UTIs. These techniques will be broadly applicable to measure *in vivo* growth rates of other bacterial pathogens during host colonization.

KEYWORDS ABU, ExPEC, PTR, UPEC, UTI, *in vivo* growth, plasmid segregation

The urinary tract is the most common site of bacterial infection in humans (1). It has been estimated that at least 40 to 50% of women will experience a minimum of one symptomatic urinary tract infection (UTI) during their lifetime, with roughly 27 to 48%

Received 24 January 2018 Accepted 26 January 2018 Published 6 March 2018

Citation Forsyth VS, Armbruster CE, Smith SN, Pirani A, Springman AC, Walters MS, Nielubowicz GR, Himpf SD, Snitkin ES, Mobley HLT. 2018. Rapid growth of uropathogenic *Escherichia coli* during human urinary tract infection. *mBio* 9:e00186-18. <https://doi.org/10.1128/mBio.00186-18>.

Editor Jeff F. Miller, UCLA School of Medicine

Copyright © 2018 Forsyth et al. This is an open-access article distributed under the terms of the [Creative Commons Attribution 4.0 International license](https://creativecommons.org/licenses/by/4.0/).

Address correspondence to Harry L. T. Mobley, hmobley@umich.edu.

* Present address: Chelsie E. Armbruster, Department of Microbiology and Immunology, State University of New York at Buffalo, Buffalo, NY, USA; Matthew S. Walters, MMS Holdings, Inc., Canton, MI, USA; Greta R. Nielubowicz, Biological Sciences Program, Macomb Community College, Warren, MI, USA.

† Deceased.

This article is a direct contribution from a Fellow of the American Academy of Microbiology. Solicited external reviewers: Matthew Mulvey, University of Utah School of Medicine; Mark Schembri, University of Queensland.

of affected women experiencing recurrent UTIs (2). In 2007, alone, UTIs resulted in 8.6 million physician visits, with women comprising 84% of the visits (3).

Lower UTI begins with bacterial colonization of the periurethral area by fecal contamination from the gastrointestinal tract, followed by ascension of bacteria through the urethra and into the bladder, causing cystitis. Unresolved cystitis may progress to an upper UTI, termed pyelonephritis, when bacteria ascend the ureters and enter one or both kidneys (4). Pyelonephritis, in some cases, progresses to bacteremia. Thus, during the course of an infection, a successful uropathogen must navigate dramatically different niches, including the gastrointestinal tract, periurethral area, urethra, bladder, ureter, kidney, and bloodstream.

Escherichia coli is the most common cause of UTIs (1, 5), with both symptomatic and asymptomatic infections most often being associated with specific uropathogenic *E. coli* (UPEC) sublineages. To elucidate the functional capacities that differentiate UPEC strains from *E. coli* strains that have distinct tropisms (e.g., gastrointestinal commensal lineages), UPEC strains were first studied *in vitro*, leading to the identification of distinguishing phenotypes, such as adherence and hemolytic activity, that contributed to the ability of the bacterium to infect and damage the host (6, 7). To more rigorously identify genes and pathways relevant to pathogenesis, our group, and others, began to employ animal models that mimic the human disease process (8). Increasingly sensitive methods have become available and are now being applied in these animal models or in human urine to understand the processes essential for uropathogenesis. These include competition experiments (9), application of signature-tagged mutagenesis (10, 11), identification of fitness genes by transposon sequencing (Tn-seq) (12–15), and measurement of the complete UPEC transcriptome during infection by microarray and transcriptome sequencing (RNA-seq) (16–18).

While these studies have provided a mechanistic understanding of what UPEC is doing during different stages of infection, it is far less clear how these functional dynamics relate to growth dynamics. In particular, while it has now become routine to quantify virtually every gene, protein, and metabolite produced by a bacterium, it has remained a challenge to probe the bacterial growth rate *in vivo*. In addition to providing necessary context for the proper interpretation of the aforementioned omics experiments, the measurement of the *in vivo* growth rate is essential (i) to understand the temporal dynamics of the infectious cycle (i.e., to determine how fast UPEC adapts to available nutrients in the host and how its capacity for rapid growth relates to host damage), (ii) to discern growth variation occurring in different compartments and anatomical sites (i.e., to determine whether growth is more rapid in the bladder or in urine itself), and (iii) to facilitate meaningful comparisons between different strains or species that may have different growth dynamics (i.e., to determine whether there are strain-dependent differences in growth rate).

In this study, we used UPEC, asymptomatic bacteriuria (ABU), and fecal isolates to test the hypothesis that UPEC isolates adapt more quickly to nutrient availability, grow more rapidly, and better survive the innate immune response within the urinary tract than other *E. coli* isolates. We employed two independent methods to assess the growth rate during infection: plasmid segregation and a sequencing-based method that enumerates bacterial chromosomal replication forks as a function of growth rate, known as the peak-to-trough ratio (PTR). We demonstrate that UPEC strains rapidly divide in both the murine and human urinary tracts and survive in the host.

RESULTS

Bladder colonization in the murine model is similar between *E. coli* isolates at 6 h, but fecal strains survive poorly 48 h postinoculation. To test the hypothesis that UPEC isolates differentially establish and maintain infection in the urinary tract compared to fecal and ABU strains, we transurethrally inoculated C57BL/6 mice with 10^8 CFU of 11 different *E. coli* strains representing UPEC (3 strains), ABU (4 strains), and fecal (4 strains) isolates. CFU per gram of bladder were determined 6 h postinoculation (hpi) (Fig. 1A). Every mouse was colonized, with median bladder values ranging from

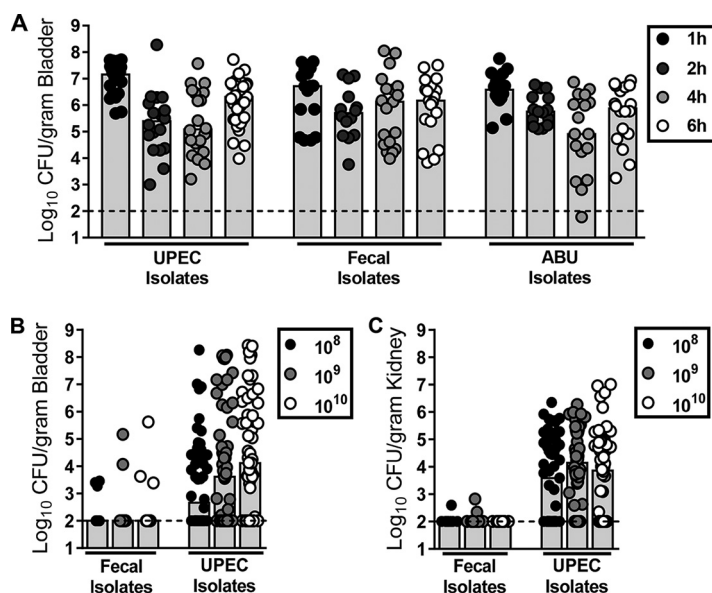


FIG 1 UPEC, fecal, and asymptomatic strains colonize the murine bladder at 6 hpi. (A) Bacterial recovery from bladders of mice transurethraly inoculated with 10^8 CFU/ml UPEC (CFT073, UT189, 536), fecal (EFC1, EFC2, EFC4, and EFC7), or ABU (PUTS37, PUTS58, PUTS59, and ABU83972) strains. Infections proceeded for 1 h (black circles), 2 h (dark gray circles), 4 h (light gray circles), or 6 h (open circles). (B and C) Bacterial recovery from the bladder (B) and kidneys (C) of mice transurethraly inoculated with 10^8 (black circles), 10^9 (gray circles), or 10^{10} (open circles) CFU/ml of fecal (EFC4 and EFC7) or UPEC (F3, F15, F11, F24, F54, CFT073, CFT269, CFT189, CFT204, and CFT325) isolates. Bladder and kidneys were harvested at 48 hpi. In panels A, B, and C, symbols represent individual mice and bars represent the median. $n = 4$ to 60. The limit of detection is 100 CFU/g. As an index of type 1 fimbrial expression, strain CFT073 agglutinated a suspension of yeast (*Saccharomyces cerevisiae*) at a bacterial titer of 1:32. Strains ABU83972 and EFC7 failed to agglutinate yeast. Colonization and virulence gene data for each strain may be found in Fig. S1.

7.6×10^5 to 2.0×10^6 CFU/g bladder. Thus, the fecal, UPEC, and ABU strains examined in this study can all survive in the urinary tract for at least 6 hpi.

Since it has been demonstrated that UPEC strains carry more virulence determinants than fecal strains (19, 20) (see Fig. S1 in the supplemental material) and cause persistent infections, whereas fecal strains do not, we transurethraly inoculated mice with either fecal or UPEC strains with inocula of 10^8 , 10^9 , or 10^{10} CFU. After 48 h, bladder bacterial burden was enumerated. All three inoculum concentrations resulted in bladder colonization by the UPEC isolates up to $\sim 10^8$ CFU/g bladder; however, fecal strains survived poorly, with median values below the limit of detection of 100 CFU/g (Fig. 1B). Kidney colonization (Fig. 1C) was reflective of bladder colonization. These results indicated that fecal strains are unable to persist out to 48 hpi in the murine urinary tract following transurethral challenge, regardless of the inoculating dose. While resistance to the innate immune response, particularly neutrophil infiltration, may explain UPEC's ability to colonize the urinary tract more successfully than fecal strains (21, 22), it is also possible that persistence may relate to the bacterial growth rate within urine and the host environment. For this reason, we sought to measure the bacterial growth rate within the urinary tract.

***In vivo* doubling time for ABU strains is statistically longer than those for UPEC and fecal strains via plasmid partitioning.** We utilized pGTR902, which replicates in the presence of L-arabinose (23), for estimation of bacterial growth rate in a collection of UPEC, fecal, and ABU isolates in the murine model of ascending UTI. To assess the growth rate, pGTR902 was introduced into UPEC isolate CFT073 by electroporation and cultured in LB medium with and without 1% L-arabinose. The total number of bacteria was enumerated by plating on LB agar, and the number harboring pGTR902 was determined by plating on LB agar containing kanamycin and L-arabinose. The presence of pGTR902 did not affect growth of CFT073 in LB broth with or without L-arabinose, and a decrease in the number of CFT073 cells containing pGTR902 was only observed

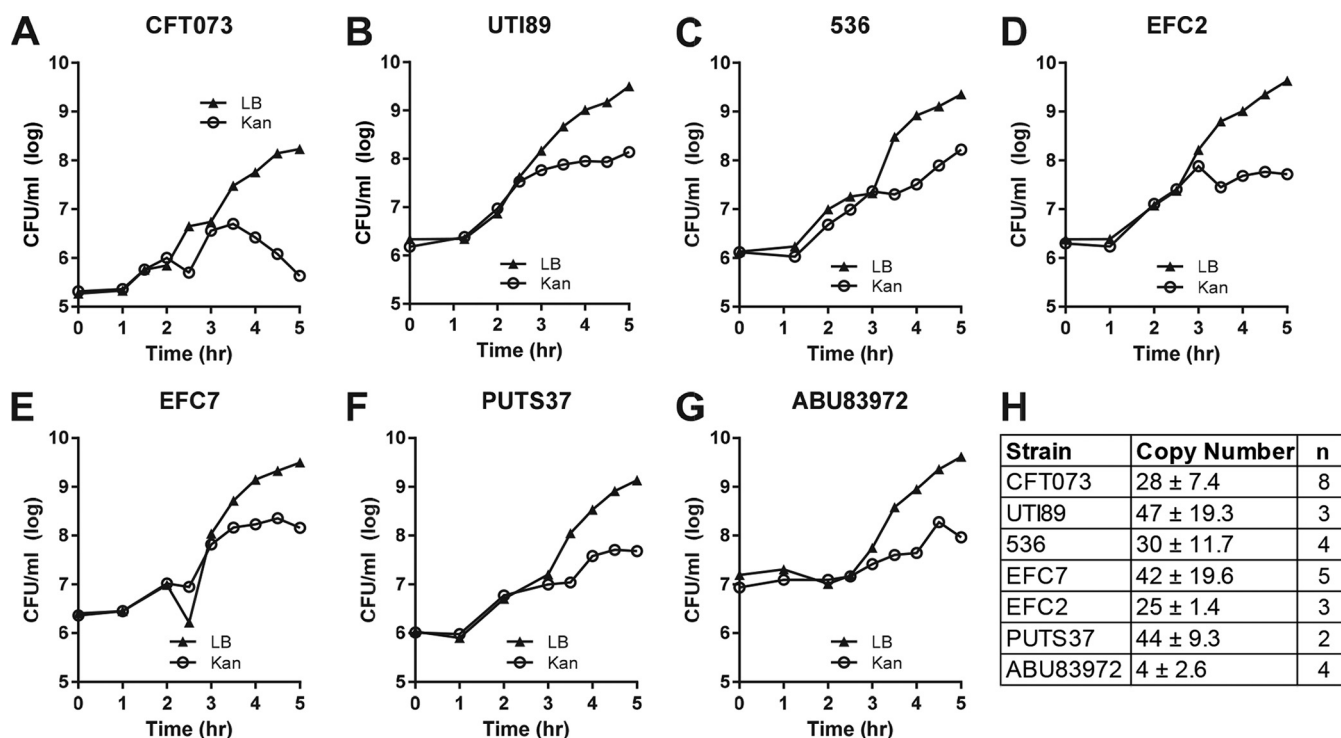


FIG 2 pGTR902 copy number is variable among EXPEC isolates. (A to G) Representative growth curves in LB diluted 1:100 (ABU83972) or 1:1,000 (CFT073, UTI89, 536, EFC2, EFC7, and PUTS37) from overnight cultures grown in LB supplemented with 1% L-arabinose and kanamycin (25 μg/ml). Cultures were grown at 37°C with aeration, and CFU per milliliter of pGTR902-containing bacteria and total bacteria (bacteria containing and those not containing pGTR902) were determined at 30-min or 1-h intervals by plating on LB agar containing 1% L-arabinose and kanamycin (25 μg/ml) (open symbols) and LB agar containing no antibiotic (closed symbols), respectively. (H) The copy number of pGTR902 in each isolate was calculated using the following equation: CFU/ml of pGTR902-containing bacteria at stationary phase/CFU/ml of pGTR902-containing bacteria in the inoculum. Values are mean ± standard deviation.

in LB medium lacking L-arabinose (see Fig. S2 in the supplemental material). Comparisons between strains require precise determination of pGTR902 copy number in each strain. We therefore introduced pGTR902 into two additional UPEC isolates (UTI89 and 536), two fecal isolates (EFC7 and EFC2), and two ABU isolates (PUTS37 and ABU83972) and conducted *in vitro* growth experiments in LB medium without L-arabinose to calculate plasmid copy number based on plasmid segregation (Fig. 2). Plasmid segregation was observed in all seven strains (Fig. 2A to G), and average copy number was determined from 2 to 8 independent experiments per strain by dividing the number of pGTR902-containing bacteria at stationary phase by the number of pGTR902-containing bacteria present in the inoculum (Fig. 2H). Copy numbers differed between *E. coli* isolates, ranging from approximately 4 plasmids per bacterial cell in ABU83972 to approximately 47 plasmids per bacterial cell in UTI89. Plasmid segregation and copy number for CFT073, EFC7, and ABU83972 cultured in human urine were similar to that attained in LB (compare Fig. S3A to C in the supplemental material to Fig. 2A, E, G), suggesting that pGTR902 may segregate similarly within the urinary tract.

To estimate growth rate *in vivo*, C57BL/6 mice were transurethrally inoculated with 10⁸ CFU/mouse of each *E. coli* isolate harboring pGTR902. Six hours postinfection was chosen as the ideal time point to harvest bladders for CFU as all seven isolates colonized to similar levels at this time (Table 1; see Fig. S4 in the supplemental material). Growth proportion, number of generations, and *in vivo* doubling time were estimated for each *E. coli* strain using total CFU recovered from the bladder of each mouse, the CFU of pGTR902-containing bacteria, and the experimentally determined plasmid copy number (Table 1). The *in vitro* doubling time of each strain during logarithmic growth in LB medium is shown for comparison. Overall, there were no statistically significant differences in bladder colonization, growth proportion, number of generations, or doubling time between each of the seven isolates. However, the

TABLE 1 Plasmid segregation as a method to estimate doubling time

Strain	Bladder log ₁₀ CFU ^a	Growth proportion ^b	No. of generations ^c	Doubling time (min)	
				<i>In vivo</i> ^d	<i>In vitro</i> ^e
UPEC isolates					
CFT073	6.6 ± 1.4	-3.6 ± 1.5	11.9 ± 5.0	36.3 ± 15.6	32.0 ± 4.8
UTI89	6.4 ± 0.5	-2.8 ± 0.6	9.3 ± 2.1	40.5 ± 8.7	26.5 ± 3.2
536	6.3 ± 0.7	-2.9 ± 0.5	9.6 ± 1.5	38.4 ± 6.3	28.0 ± 2.1
Avg	6.5 ± 1.1	-3.3 ± 1.3	11.0 ± 4.2	37.5 ± 13.2	29.4 ± 4.3
Fecal isolates					
EFC7	5.5 ± 0.6	-2.2 ± 0.6	7.1 ± 1.9	60.8 ± 3.3	27.5 ± 0.2
EFC2	6.0 ± 1.4	-2.4 ± 0.6	8.1 ± 2.0	46.5 ± 10.5	26.2 ± 0.4
Avg	5.8 ± 1.2	-2.3 ± 0.6	7.8 ± 1.9	53.7 ± 10.1	26.7 ± 0.8
ABU isolates					
PUTS37	5.8 ± 0.6	-2.1 ± 0.3	6.9 ± 1.1	53.0 ± 9.0	30.5 ± 1.1
ABU83972	4.2 ± 0.7	-1.3 ± 0.8	4.3 ± 2.7	112.6 ± 58.3	43.8 ± 17.9
Avg	5.0 ± 1.0	-1.7 ± 0.7	5.6 ± 2.4	82.8 ± 50.3 ^f	39.4 ± 15.5

^aC57BL/6 mice were transurethrally inoculated with 10⁸ CFU/mouse of each isolate harboring pGTR902. Bladders were harvested 6 h postinoculation for enumeration of total bacterial CFU and plasmid-containing CFU. Values are reported as the mean log₁₀ CFU per gram of bladder tissue ± standard deviation for 4 to 21 mice per isolate.

^bGrowth proportion was calculated as follows: (log₁₀ CFU/g of plasmid-containing bacteria/plasmid copy no.) - log₁₀ total CFU/g.

^cThe number of generations for logarithmic bacterial growth *in vivo* was calculated as follows: growth proportion/−0.301.

^dThe doubling time for *in vivo* growth was calculated as follows: time postinoculation (min)/no. of generations.

^eThe doubling time *in vitro* during growth in LB was calculated as follows: time postinoculation (min)/[(3.3 × log₁₀ CFU at inoculation)/log₁₀ CFU at time postinoculation (min)].

^f*P* < 0.0001 compared to UPEC and fecal isolates *in vivo* and ABU isolates *in vitro* by two-way analysis of variance (ANOVA) with Tukey test for multiple comparisons.

average *in vivo* doubling time for the ABU group was statistically longer than the average for UPEC or fecal strains (*P* < 0.0001). Indeed, CFT073 and ABU83972 are the fastest- and slowest-growing strains, respectively, of all those tested using the plasmid segregation method. No significant differences in doubling time were observed *in vitro*. We conclude from this method that UPEC and fecal strains are capable of similarly high rates of growth within the mouse urinary tract, while ABU isolates exhibit longer doubling times *in vivo* than *in vitro*.

Growth rate of CFT073 in human urine correlates with PTR. As a second method to validate measurement of *in vivo* growth rate, we determined PTR. The assay is based on the principal that a rapidly growing bacterium will initiate multiple forks of replication about the origin of replication compared to the terminus of replication to keep pace with the rate of bacterial division. Thus, a faster-growing bacterium will have a higher PTR than a slower-growing bacterium (24). To test the technique, UPEC strain CFT073 was cultured with aeration in media that support different growth rates: M9 salts supplemented with 0.4% glucose, LB medium, and Terrific broth. Bacteria were collected during the mid-exponential phase of growth for each medium. Genomic DNA was isolated and subjected to Illumina sequencing. Sequence reads were aligned to the genomic sequence of CFT073 (Fig. 3A) (25). PTR was calculated using the following equation: % of reads at the origin/% of reads at the terminus. High PTR values were calculated for bacteria growing in rich media (LB medium and Terrific broth) (PTR = 1.62, 40.5-min doubling time, and PTR = 1.68, 40.0-min doubling time, respectively), and a low PTR value was calculated for bacteria growing in minimal medium (M9 salts supplemented with 0.4% glucose) (PTR = 1.27, 54.2-min doubling time) (Fig. 3A). As expected, bacteria growing rapidly in rich media display higher PTRs than bacteria growing slower in minimal medium.

Before determining the PTR of CFT073 *in vivo*, we first calculated the PTR of CFT073 cultured in pooled human urine. As expected, PTR values were high during the exponential phase and decreased in a stepwise fashion as the culture approached and entered the stationary phase (Fig. 3B and C). These data were used to construct a standard curve that correlated growth rate as measured by optical density at 600 nm (OD₆₀₀) with PTR calculated at 3, 4, 5, 6, 7, and 8 h (Fig. 3D). A near perfect correlation

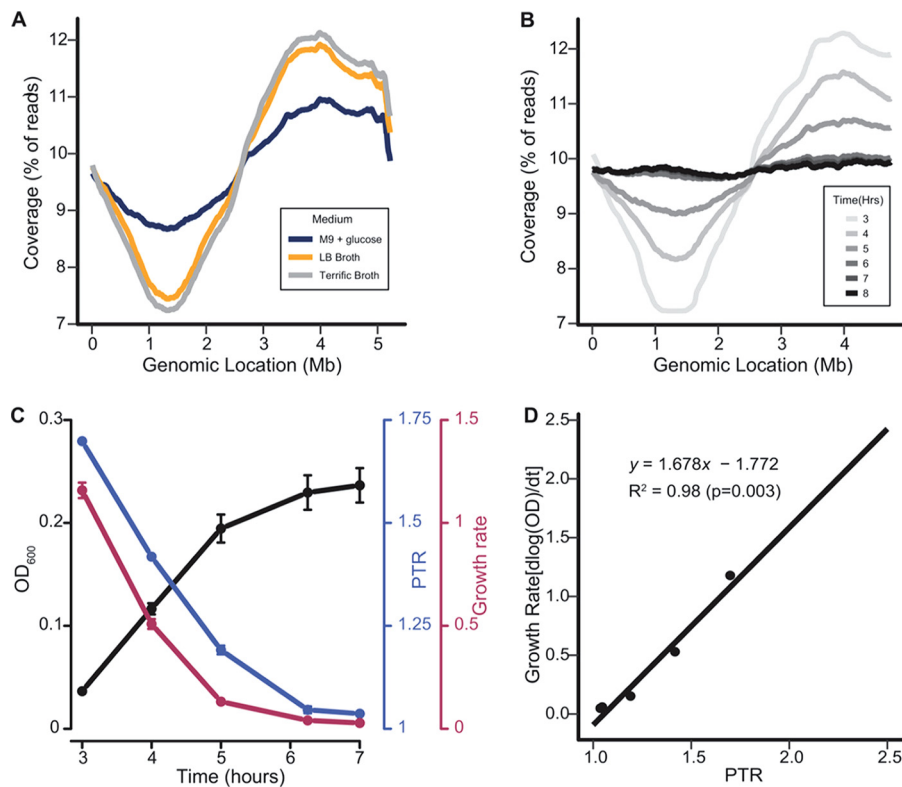


FIG 3 Growth rate is correlated with PTR *in vitro*. (A) *E. coli* CFT073 was inoculated into M9 supplemented with 0.4% glucose (blue), LB (yellow), and Terrific broth (gray) and grown to the mid-exponential phase (OD_{600} of 0.25, 0.55, and 0.67, respectively). DNA sequencing reads from each sample were aligned to the CFT073 chromosome (x axis), and the average coverage across the chromosome was calculated for replicate pairs (y axis). (B) DNA sequencing reads obtained from CFT073 grown in human urine were aligned to the CFT073 genome as in panel A. Average coverage from paired replicates is shown. (C) Triplicate OD_{600} measurements (black) at the corresponding time points from panel B. Growth rates (red) were calculated as the logarithm of the change in OD. PTR values (blue) from panel B are shown. Symbols represent the average, and bars represent the standard deviation. (D) A linear model was constructed using PTR and the

of growth rate with PTR was observed ($R^2 = 0.98$), allowing extrapolation of doubling time from a given PTR value.

***E. coli* CFT073, ABU83972, and EFC7 have differential growth rates over time in the mouse model of UTI, as measured using PTR.** Mice were transurethrally inoculated with 10^8 CFU *E. coli* CFT073. The urine and bladder samples of each mouse were collected at 6, 24, and 30 hpi. Bacteria were harvested from pooled urine ($n = 4$) by centrifugation, and genomic DNA was extracted. Bladder samples from individual mice were homogenized and enriched for bacterial cells using differential lysis (see Fig. S5 in the supplemental material), and DNA was isolated. DNA from urine and bladder preparations was subjected to Illumina sequencing. Enrichment of bladder homogenates for bacterial genomic DNA was critical to ensure that the threshold for accurate PTR determination, $\geq 0.2 \times$ genome coverage (see Fig. S6 in the supplemental material), was met. Treatment of bladder homogenates with mammalian cell lysis buffer had only a modest effect on bacterial viability compared to phosphate-buffered saline (PBS)-treated controls (see Fig. S7 in the supplemental material). PTR values determined for murine bladders ($n = 3$ to 4) predicted a high growth rate (PTR = 1.78, 36.9 ± 3.8 -min doubling time) at 6 hpi, slowing at 24 hpi (PTR = 1.21, 160 ± 27 -min doubling time) and 30 hpi (PTR = 1.22, 167 ± 70 -min doubling time) (Fig. 4A and C). Similarly, urine PTR values indicated a high growth rate (PTR = 1.75, 34.9 -min doubling time) at 6 hpi, which slowed dramatically at 24 hpi (PTR = 1.09; 797 -min doubling time) and 30 hpi (PTR = 1.10; 618 -min doubling time) (Fig. 4B and C). The increasing fraction of

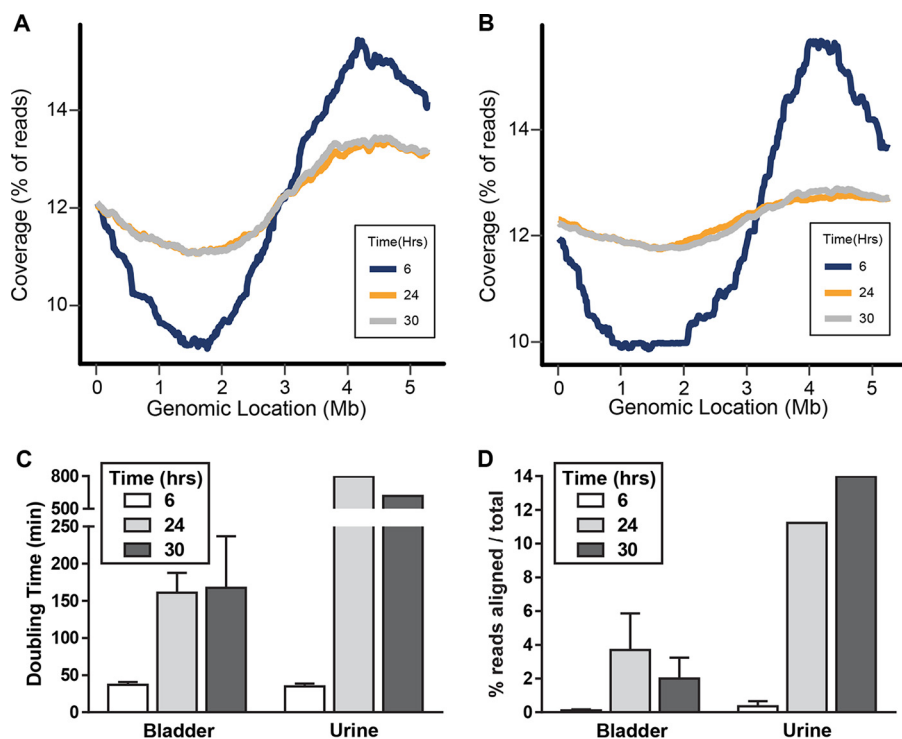


FIG 4 UPEC strain CFT073 growth is rapid at early time points during murine UTI. Mice were transurethraly inoculated with 10^8 CFU/ml of *E. coli* CFT073. At 6 h (blue), 24 h (yellow), or 30 h (gray) postinoculation, bladder (A) and pooled urine (B) samples were processed to enrich for bacterial genomic DNA. DNA sequencing reads were aligned to the CFT073 genome (x axis), and the coverage across the chromosome was calculated (y axis). $n = 3$ to 4. (C) Doubling times for CFT073 in bladder and urine (y axis) were extrapolated using the formula from Fig. 2D. $n = 3$ to 4. Twenty-four-hour and 30-h urine samples from four mice were pooled for PTR determination. (D) The percentage of sequence reads from urine or bladder samples aligned to the CFT073 genome is shown (y axis) for the samples in panel C.

sequence reads homologous to CFT073 at 24 and 30 hpi suggests that the bacteria reach a saturating population size within the nutrient-limited urinary tract, leading to decreased growth (Fig. 4D). This hypothesis is supported by an increase in bacterial load from $\sim 10^6$ CFU/g bladder at 6 hpi to $\sim 10^8$ CFU/g bladder at 24 hpi (see Fig. S8 in the supplemental material). An additional observation is the marked increase in the doubling time of the inoculum compared to the doubling time in the bladder at 6 hpi (119 min versus 36.9 min, respectively), indicating rapid adaptation of UPEC strain CFT073 to conditions within the murine host.

PTR values were also calculated for ABU strain ABU83972 and fecal strain EFC7 during murine UTI. However, because the ABU and fecal strain bacterial burden was not sufficient ($<10^4$ CFU/g bladder [Fig. S8]) to obtain the genome coverage level required for the most accurate PTR determination, we can only define trends in growth rate. In contrast to CFT073, ABU83972 tended to maintain a relatively high growth rate in the bladder at 6, 24, and 30 hpi, with doubling times of 37, 31, and 47 min, respectively. Fecal strain EFC7 was found to have a moderately longer doubling time in the urine (72 min) at 6 hpi compared to ABU83972 and CFT073. Similarly, a modest increase in doubling time in the bladder was observed at 24 and 30 hpi (84 and 67 min, respectively) compared to 6 hpi (46 min). These results indicate that neither EFC7 nor ABU83972 reaches saturation in the bladder, yet ABU83972 maintains a high growth rate at 24 and 30 hpi, while EFC7 replicates more slowly at 24 and 30 hpi.

PTR indicates rapid growth of UPEC isolates during human UTI. By standardizing PTR measurement *in vitro* in human urine and *in vivo* using the mouse model, it was possible to estimate the growth rate of *E. coli* strains during uncomplicated UTI in women. Genomic DNA was extracted from urine that had been previously collected

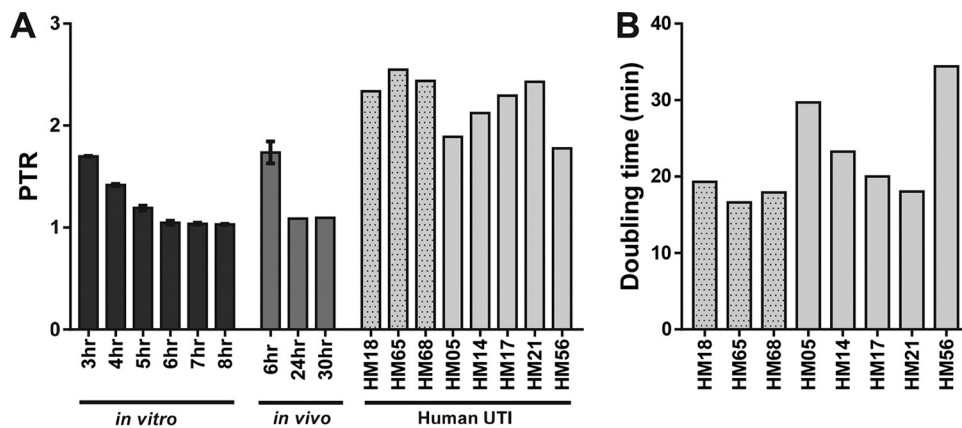


FIG 5 PTR of UPEC during human UTI is increased compared to *in vitro* growth or growth during murine UTI. (A) *E. coli* CFT073 containing pGTR902 grown *in vitro* in LB with 1% L-arabinose and kanamycin (25 μ g/ml) was pelleted, washed in PBS, and diluted 1:1,000 into pooled human urine. Samples were taken hourly (3 to 8 h) and subjected to Illumina sequencing, and PTRs were calculated. $n = 2$. To calculate *in vivo* PTRs, mice were transurethrally inoculated with 10^8 CFU/ml *E. coli* CFT073 containing pGTR902. The PTR of the inoculum of murine infection was 1.3, and the doubling time was 119 min. At 6, 24, or 30 hpi, bacterial genomic DNA from urine was sequenced. $n = 4$. PTRs of human urinary tract infections were calculated from bacterial genomic DNA harvested directly from infected human urine. (B) Doubling time (in minutes) extrapolated from the PTR of *E. coli* strains isolated during human UTI. In panels A and B, stippled bars represent individuals with no history of UTI. Each bar represents the mean. Error bars represent standard deviation.

(and immediately stabilized with RNAprotect) from 38 female patients with significant *E. coli* bacteriuria ($>10^5$ CFU/ml urine) and symptoms of cystitis and subjected to Illumina sequencing. Eight of these samples contained sufficient read coverage for analysis (see Fig. S9 in the supplemental material).

PTR values ranged from 1.78 to 2.55, averaging 2.23 ± 0.28 (Fig. 5A), which corresponds to very rapid doubling time estimates ranging from 16.6 to 34.4 min, averaging 22.4 ± 6.4 min (Fig. 5B). While it did not escape our notice that these rates approached maximal growth rates for any *E. coli* strain under optimal *in vitro* culture conditions, the findings nevertheless indicate that *E. coli* strains are growing at surprisingly high rates during human infection of the urinary tract and faster than that for UPEC strain *E. coli* CFT073 during *in vitro* growth in human urine (36.0 ± 2.6 min) or within the mouse urinary tract (36.9 ± 3.8 min at 6 hpi). Isolates from women with a primary UTI (stippled bars) tended to have a shorter doubling time than isolates from women who suffered from recurrent UTI (plain bars) (Fig. 5B). However, this difference was not statistically significant ($P = 0.19$).

DISCUSSION

Uropathogenic *E. coli* cells divide rapidly in both the murine and human urinary tracts, as measured by both a plasmid segregation method (mice only) and PTR (both mice and humans). At early time points postinoculation, ABU strains may be reliant on growth rate alone to successfully colonize as they often lack adhesins. Fecal strains, in general, do not carry a significant number of virulence determinants (19, 20) and did not colonize well at time points beyond 6 hpi. UPEC strains are relatively resistant to killing by the innate immune response at 48 h, as indicated by high bacterial loads recovered from the bladder over the entire time course of the infection studies. For the human studies, while we do not know precisely when *E. coli* entered the bladder, and thus the “hours postinoculation” are unknown, growth is uniformly rapid. These results suggest that UPEC strains are metabolically suited to grow rapidly in the urine within the bladder, even in the presence of a robust innate immune response. Indeed, damage to the host during infection, inflicted both by the bacterium and the host inflammatory response, likely releases additional nutrients to fuel this rapid growth.

We employed two techniques to measure growth rate *in vivo*. The first method followed plasmid segregation of a nonreplicating plasmid, pGTR902, developed for

estimation of the growth rate of *Vibrio vulnificus* in skin lesions (23). One advantage of this technique is the ease of use in all *E. coli* strains tested. *E. coli* isolates transformed with plasmid pGTR902 were cultured *in vitro* in the presence of arabinose to drive replication of the plasmid and then washed and transurethrally inoculated into the murine urinary tract in which arabinose is absent. Rapid results were obtained within 24 h by plating on agar with and without L-arabinose and kanamycin to allow for differential enumeration of plasmid-containing bacteria. Limitations of the plasmid segregation method include the fact that it cannot be used in naturally occurring infections as the method requires experimental parameters to be defined. In addition, there is potential skewing of growth rate estimation if the plasmid does not properly segregate *in vivo* or if plasmid-containing bacteria are eliminated during infection.

The second method for determination of growth rate *in vivo* measured the peak-to-trough ratios for genomic DNA from *E. coli in vitro* or *in vivo*. This is a powerful tool for estimation of growth rate in an open system like the urinary tract and will not be skewed by loss of bacteria due to urination or ascension to the kidneys. It allows for estimation of bacterial growth rate in naturally occurring infections, not just experimental models. The limitations of the technique are that it is expensive and time-consuming compared to CFU determination. It requires sufficient read depth to accurately assess growth rate and requires assembly of reads on a genome scaffold (i.e., the strain's genome must have been sequenced and assembled). Also, PTR estimates the average value for all bacteria in urine whether they are truly planktonic, adherent to exfoliated epithelial cells, or dead with genomic DNA undamaged.

Determinations for growth rates by the plasmid segregation method and PTR at 6 h postinoculation in the murine model agree well, with one notable exception. The doubling times for pyelonephritis strain *E. coli* CFT073 in the bladder were measured at 36.3 and 36.9 min by plasmid segregation and PTR, respectively. Indeed, the values were nearly identical. Values for UPEC type strains CFT073, UTI89, and 536 were also similar at 6 h in the bladder by plasmid segregation at 36.3, 40.5, and 38.4 min doubling times (average of 37.5 min), respectively. The latter strains (UTI89 and 536) were not tested by PTR. The growth rate of fecal strain *E. coli* EFC7 was slower than that of CFT073, with similar doubling times in the bladder of 60.8 and 46 min, as assessed by plasmid segregation and PTR, respectively. On the contrary, asymptomatic bacteriuria strain *E. coli* ABU83972 had estimated doubling times of 113 and 37 min by plasmid segregation and PTR, respectively. The reason for this dramatic difference is unclear but could be due to increased plasmid stability in the ABU strain versus those in the UPEC and fecal strains tested.

Using the plasmid segregation and PTR techniques, we were able to answer fundamental questions about UPEC biology in the urinary tract. For example, can we understand the temporal dynamics of the infectious cycle? That is, how fast does UPEC adapt to nutrient availability within its host? In a mouse inoculated with an overnight culture grown in LB, the doubling time was 119 min at the time of inoculation. Six hours after inoculation, the growth rate in the bladder increased to 36.9 min as it adapted to growth *in vivo*. This doubling time was consistent with estimates of 30 to 35 min in the first 8 h within intracellular bacterial communities (IBCs) within the bladders of mice experimentally infected with UPEC strain UTI89 (26). Surprisingly, despite the fact that fresh urine is constantly synthesized in the kidney and delivered to the bladder, thus refreshing the growth medium, *E. coli* appears to enter a stationary growth-like phase with slow doubling times by 24 hpi (161 min) and 30 hpi (167 min). During human infection, *E. coli* cells grow in the gastrointestinal tract and then contaminate the periurethral area and ascend the urethra to the bladder, and symptoms of cystitis are elicited between 24 h and 3 days postinoculation of the bladder (27, 28). It is at this point in the infection cycle that urine was collected from human patients, and PTR values were consistent with extraordinarily rapid growth (mean doubling time of 22.4 min). Thus, the human bladder appears to act more like a chemostat in which medium (urine) is refreshed constantly and outflow is accomplished by frequent urination. In the mouse bladder, urine may not be refreshed as rapidly as necessary to

maintain exponential growth. This may reflect a fundamental difference between the murine model and human infection.

Differences in growth dynamics in the murine and human urinary tracts may also help explain differences in the expression of phase-variable type 1 fimbriae during infections in mice and humans. Selection for expression of these fimbriae is observed both under conditions of reduced oxygen and in the stationary phase of growth (29). Indeed, type 1 fimbriae are expressed during experimental murine UTI (30, 31), especially late in infection. This would be consistent with UPEC growth entering stationary phase at high CFU ($\sim 10^8$ CFU/g), likely due to limiting oxygen availability. On the other hand, several studies have found the orientation of the *fim* promoter is more often in the “off” position when examined directly from the urine of infected women (17, 18, 32). That *E. coli* cells examined in the urine collected and stabilized immediately have growth rates consistent with exponential growth may explain why a substantial percentage of the isolates are not expressing type 1 fimbrial genes during the human infections. Higher oxygen tension in the human bladder compared to the mouse bladder may also help to explain this, but has not been measured.

We can also ask whether there is growth variation occurring in different anatomical sites. When PTR values during murine infection were compared between the urine and the bladder for UPEC strain CFT073, similar doubling times were observed at 6 hpi (34.9 and 36.9 min, respectively); however, at 24 and 30 hpi, doubling times were dramatically longer in the urine than in the bladder. Given that PTR measures the average of all bacteria whether planktonic, adherent, or intracellular, bacteria in the bladder are replicating faster beyond 6 hpi. It is possible that concentrations of nutrients are higher in the bladder at later time points due to damage to the epithelium by the action of bacterial cytotoxicity and the process of inflammation.

Further, we may ask if meaningful comparisons can be made between strains with potentially different growth dynamics. We know well that UPEC strains display tremendous heterogeneity with respect to genes present in pathogenicity islands beyond the conserved base genome found in commensal strains (19, 20, 33). Indeed, this heterogeneity is displayed by the strains from women with symptoms of cystitis (17). Sequencing of these strains (34) revealed differences in genome size and the presence of a wide variety of accessory genes necessary to colonize the urinary tract (i.e., different combinations of adhesins, iron acquisition systems, and toxins). Consequently, the human UPEC strains displayed variation in growth in human urinary tract infection (Fig. 5). Indeed, expression of type 1 fimbriae may provide an alternative explanation for the differences observed in bladder colonization between strain types. Fecal strain EFC7 and asymptomatic strain ABU83972 do not agglutinate yeast (data not shown), indicative of a lack of expression of functional type 1 fimbriae.

E. coli transcriptome profiles from the urine of patients with urinary tract infection, described in three reports using either microarray technology (18) or RNA sequencing (17, 35), are consistent with the ability to achieve rapid bacterial growth *in vivo* compared to *in vitro* culture (Fig. 5). In one study from urology clinic patients with *E. coli* bacteriuria (18), the most highly expressed bacterial genes in urine were those encoding ribosomal protein subunits. Ribosomal genes represented between 24 and 54% of the top 50 upregulated genes for the eight *E. coli* isolates compared to gene expression by the same isolates in LB cultures. Selected nonribosomal genes, upregulated during UTI, were also consistent with rapid growth *in vivo*, including those required for translation, the F_0F_1 ATPase, fatty acid biosynthesis, and protein folding and secretion. *E. coli* from the urine of elderly patients with UTI (35) upregulated 202 genes compared to *in vitro* culture in rich medium. Twenty percent of these upregulated genes were involved in translation (ribosomal protein genes) or ATP synthesis, all indicative of rapid growth. Finally, in a transcriptome study of *E. coli* in the urine of patients with uncomplicated cystitis (17), similar genes, including those encoding ribosomal proteins, were highly upregulated during infection compared to *in vivo* growth in human urine or LB medium.

We have shown that the mean PTR value from *E. coli* strains collected during active

uncomplicated UTIs is 2.0 ± 0.5 (Fig. 5A). Although this value reflects a very high growth rate and exceeds the range of PTR values obtained *in vitro* used to establish a standard curve (Fig. 3), it does not exceed the range of PTR values found in previous studies. Korem et al. reported a PTR of 2.6 for commensal *E. coli* (K-12 NCM 3722) during the exponential phase *in vitro* and PTR values ranging from 1 to 2.6 for *E. coli* in human fecal samples (36). One study comparing the growth rate of *E. coli* strains on infant skin, mouth, and gut samples found PTR values ranging from 0.9 to 2.2, with PTR values in the skin and mouth significantly higher than in the gut (37). Brown et al. found *E. coli* in the gut of a premature infant having a PTR of 1.91. In the same study, PTR values for all species present ranged from 1.2 to 2.6 in the premature infant microbiome and 1.1 to 2.1 in the adult microbiome (38). Thus, our reported PTR values for UPEC in human UTI are within the bounds of published microbiome studies.

Certainly, future questions remain. For example, do UPEC strains persist by employing immune evasion or altering metabolic strategy at later time-points? What prevents UPEC strains in humans from progressing to a systemic infection with higher frequency than is observed clinically given the high growth rate calculated here? In all, however, this study highlights the use of PTR to estimate relative rates of growth in murine and human urinary tract infections and reveals that uropathogenic *E. coli* strains are replicating at a surprisingly high rate during human infection. This technique should be widely applicable for measurement of bacterial growth rates during infection.

MATERIALS AND METHODS

Extended materials and methods can be found in Text S1 in the supplemental material.

Ethics statement. Urine collection was approved by the University of Michigan Institutional Review Board (HUM00004949). Informed consent for collection of urine specimens from women attending the University Health Services was approved by the Michigan Institutional Review Board (HUM00029910) (17). All animal protocols were approved by the Institutional Animal Care and Use Committee (IACUC) at the University of Michigan Medical School (PRO00005052).

Bacterial strains, plasmids, and culture conditions. *E. coli* UPEC strains CFT073 (39), UT189 (40), and 536 (41), commensal fecal strains (EFC1, EFC2, EFC4, and EFC7 [39]), and asymptomatic bacteriuria strains (PUTS37, PUTS58, PUTS59 [42], and ABU83972 [43]) were used in this study. Genomic DNA of eight UPEC strains (HM05, HM14, HM1, HM18, HM21, HM56, HM65, and HM68) was isolated from the urine of women with cystitis and sequenced. Strains were cultured in LB broth, Terrific broth, M9 minimal medium, or LB agar.

Segregation of plasmid pGTR902 *in vitro*. Plasmid pGTR902, transformed into *E. coli* strains, was used to estimate growth rate as previously described (23).

Murine model of ascending UTI. Six- to eight-week-old female C57BL/6 mice (Envigo) were infected as previously described (44, 45).

Segregation of plasmid pGTR902 *in vivo*. Bacteria transformed with plasmid pGTR902 were cultured overnight with 1% arabinose and kanamycin (25 $\mu\text{g}/\text{ml}$), harvested, and washed. A total of 10^8 CFU were transurethraly inoculated into the mouse bladder. At 6 hpi, bladders and kidneys were removed, homogenized, and plated onto LB agar with and without 1% L-arabinose and kanamycin (25 $\mu\text{g}/\text{ml}$). The calculations used to determine the *in vivo* number of generations have been described previously (23). We have made the logical extension of these calculations to determine the doubling time.

Estimation of *in vitro* and *in vivo* growth rates via PTRs. Genomic DNA, isolated from bacteria harvested from culture medium, bladders, and urine of infected mice and bacteria in the urine of women with *E. coli* bacteriuria, was subjected to Illumina sequencing. PTRs were calculated using the peak and trough location with maximum and minimum values from the resulting smoothed coverage (36, 46–48).

SUPPLEMENTAL MATERIAL

Supplemental material for this article may be found at <https://doi.org/10.1128/mBio.00186-18>.

TEXT S1, DOCX file, 0.1 MB.

FIG S1, TIF file, 9.6 MB.

FIG S2, TIF file, 7.8 MB.

FIG S3, TIF file, 4.2 MB.

FIG S4, TIF file, 10.6 MB.

FIG S5, TIF file, 8.7 MB.

FIG S6, TIF file, 11.8 MB.

FIG S7, TIF file, 13.5 MB.

FIG S8, TIF file, 7.9 MB.

FIG S9, TIF file, 11.8 MB.

ACKNOWLEDGMENTS

We thank Paul Gulig for the generous gift of plasmid pGTR902.

This work was supported by Public Health Service grants AI059722 and DK094777 from the National Institutes of Health to H. L. T. Mobley. The content may not represent the official views of the National Institutes of Health.

REFERENCES

1. Foxman B. 2014. Urinary tract infection syndromes: occurrence, recurrence, bacteriology, risk factors, and disease burden. *Infect Dis Clin North Am* 28:1–13. <https://doi.org/10.1016/j.idc.2013.09.003>.
2. Warren JW. 1996. Clinical presentations and epidemiology of urinary tract infections, p 3–27. *In* Mobley HLT, Warren JW (ed), *Urinary tract infections: molecular pathogenesis and clinical management*. ASM Press, Washington, DC.
3. Schappert SM, Rechtsteiner EA. 2011. Ambulatory medical care utilization estimates for 2007. *Vital Health Stat* 169:1–38.
4. Mobley HL, Donnenberg MS, Hagan EC. 21 December 2009. Uropathogenic *Escherichia coli*. *EcoSal Plus* <https://doi.org/10.1128/ecosalplus.8.6.1.3>.
5. Ipe DS, Sundac L, Benjamin WH, Jr, Moore KH, Ulett GC. 2013. Asymptomatic bacteriuria: prevalence rates of causal microorganisms, etiology of infection in different patient populations, and recent advances in molecular detection. *FEMS Microbiol Lett* 346:1–10. <https://doi.org/10.1111/1574-6968.12204>.
6. Edén CS, Hanson LA, Jodal U, Lindberg U, Akerlund AS. 1976. Variable adherence to normal human urinary-tract epithelial cells of *Escherichia coli* strains associated with various forms of urinary-tract infection. *Lancet* i:490–492.
7. Welch RA, Dellinger EP, Minschew B, Falkow S. 1981. Haemolysin contributes to virulence of extra-intestinal *E. coli* infections. *Nature* 294:665–667. <https://doi.org/10.1038/294665a0>.
8. Hagberg L, Hull R, Hull S, Falkow S, Freter R, Svanborg Edén C. 1983. Contribution of adhesion to bacterial persistence in the mouse urinary tract. *Infect Immun* 40:265–272.
9. Alteri CJ, Smith SN, Mobley HLT. 2009. Fitness of *Escherichia coli* during urinary tract infection requires gluconeogenesis and the TCA cycle. *PLoS Pathog* 5:e1000448. <https://doi.org/10.1371/journal.ppat.1000448>.
10. Buckles EL, Luterbach CL, Wang X, Lockett CV, Johnson DE, Mobley HL, Donnenberg MS. 2015. Signature-tagged mutagenesis and co-infection studies demonstrate the importance of P fimbriae in a murine model of urinary tract infection. *Pathog Dis* 73:ftv014. <https://doi.org/10.1093/femspd/ftv014>.
11. Bahrani-Mougeot FK, Buckles EL, Lockett CV, Hebel JR, Johnson DE, Tang CM, Donnenberg MS. 2002. Type 1 fimbriae and extracellular polysaccharides are preeminent uropathogenic *Escherichia coli* virulence determinants in the murine urinary tract. *Mol Microbiol* 45:1079–1093. <https://doi.org/10.1046/j.1365-2958.2002.03078.x>.
12. Subashchandrabose S, Smith SN, Spurbeck RR, Kole MM, Mobley HL. 2013. Genome-wide detection of fitness genes in uropathogenic *Escherichia coli* during systemic infection. *PLoS Pathog* 9:e1003788. <https://doi.org/10.1371/journal.ppat.1003788>.
13. Phan MD, Peters KM, Sarkar S, Lukowski SW, Allsopp LP, Gomes Moriel D, Achard ME, Totsika M, Marshall VM, Upton M, Beatson SA, Schembri MA. 2013. The serum resistome of a globally disseminated multidrug resistant uropathogenic *Escherichia coli* clone. *PLoS Genet* 9:e1003834. <https://doi.org/10.1371/journal.pgen.1003834>.
14. Wiles TJ, Norton JP, Russell CW, Dalley BK, Fischer KF, Mulvey MA. 2013. Combining quantitative genetic footprinting and trait enrichment analysis to identify fitness determinants of a bacterial pathogen. *PLoS Genet* 9:e1003716. <https://doi.org/10.1371/journal.pgen.1003716>.
15. Russell CW, Richards AC, Chang AS, Mulvey MA. 2017. The rhomboid protease GlpG promotes the persistence of extraintestinal pathogenic *Escherichia coli* within the gut. *Infect Immun* 85:e00866-16. <https://doi.org/10.1128/IAI.00866-16>.
16. Snyder JA, Haugen BJ, Buckles EL, Lockett CV, Johnson DE, Donnenberg MS, Welch RA, Mobley HL. 2004. Transcriptome of uropathogenic *Escherichia coli* during urinary tract infection. *Infect Immun* 72:6373–6381. <https://doi.org/10.1128/IAI.72.11.6373-6381.2004>.
17. Subashchandrabose S, Hazen TH, Brumbaugh AR, Himpsl SD, Smith SN, Ernst RD, Rasko DA, Mobley HL. 2014. Host-specific induction of *Escherichia coli* fitness genes during human urinary tract infection. *Proc Natl Acad Sci U S A* 111:18327–18332. <https://doi.org/10.1073/pnas.1415959112>.
18. Hagan EC, Lloyd AL, Rasko DA, Faerber GJ, Mobley HLT. 2010. *Escherichia coli* global gene expression in urine from women with urinary tract infection. *PLoS Pathog* 6:e1001187. <https://doi.org/10.1371/journal.ppat.1001187>.
19. Spurbeck RR, Stapleton AE, Johnson JR, Walk ST, Hooton TM, Mobley HLT. 2011. Fimbrial profiles predict virulence of uropathogenic *Escherichia coli* strains: contribution of Ygi and Yad fimbriae. *Infect Immun* 79:4753–4763. <https://doi.org/10.1128/IAI.05621-11>.
20. Spurbeck RR, Dinh PC, Walk ST, Stapleton AE, Hooton TM, Nolan LK, Kim KS, Johnson JR, Mobley HLT. 2012. *Escherichia coli* isolates that carry vat, fyuA, chuA, and yfcV efficiently colonize the urinary tract. *Infect Immun* 80:4115–4122. <https://doi.org/10.1128/IAI.00752-12>.
21. Agace WW, Patarroyo M, Svensson M, Carlemalm E, Svanborg C. 1995. *Escherichia coli* induces transuroepithelial neutrophil migration by an intercellular adhesion molecule-1-dependent mechanism. *Infect Immun* 63:4054–4062.
22. Haraoka M, Hang L, Freundus B, Godaly G, Burdick M, Strieter R, Svanborg C. 1999. Neutrophil recruitment and resistance to urinary tract infection. *J Infect Dis* 180:1220–1229. <https://doi.org/10.1086/315006>.
23. Starks AM, Bourdage KL, Thiaville PC, Gulig PA. 2006. Use of a marker plasmid to examine differential rates of growth and death between clinical and environmental strains of *Vibrio vulnificus* in experimentally infected mice. *Mol Microbiol* 61:310–323. <https://doi.org/10.1111/j.1365-2958.2006.05227.x>.
24. Cooper S, Helmstetter CE. 1968. Chromosome replication and the division cycle of *Escherichia coli* B/r. *J Mol Biol* 31:519–540. [https://doi.org/10.1016/0022-2836\(68\)90425-7](https://doi.org/10.1016/0022-2836(68)90425-7).
25. Welch RA, Burland V, Plunkett G, III, Redford P, Roesch P, Rasko D, Buckles EL, Liou SR, Boutin A, Hackett J, Stroud D, Mayhew GF, Rose DJ, Zhou S, Schwartz DC, Perna NT, Mobley HL, Donnenberg MS, Blattner FR. 2002. Extensive mosaic structure revealed by the complete genome sequence of uropathogenic *Escherichia coli*. *Proc Natl Acad Sci U S A* 99:17020–17024. <https://doi.org/10.1073/pnas.252529799>.
26. Justice SS, Hung C, Theriot JA, Fletcher DA, Anderson GG, Footer MJ, Hultgren SJ. 2004. Differentiation and developmental pathways of uropathogenic *Escherichia coli* in urinary tract pathogenesis. *Proc Natl Acad Sci U S A* 101:1333–1338. <https://doi.org/10.1073/pnas.0308125100>.
27. Czaja CA, Stamm WE, Stapleton AE, Roberts PL, Hawin TR, Scholes D, Samadpour M, Hultgren SJ, Hooton TM. 2009. Prospective cohort study of microbial and inflammatory events immediately preceding *Escherichia coli* recurrent urinary tract infection in women. *J Infect Dis* 200:528–536. <https://doi.org/10.1086/600385>.
28. Nicolle LE, Harding GKM, Preiksaitis J, Ronald AR. 1982. The association of urinary tract infection with sexual intercourse. *J Infect Dis* 146:579–583. <https://doi.org/10.1093/infdis/146.5.579>.
29. Lane MC, Li X, Pearson MM, Simms AN, Mobley HLT. 2009. Oxygen-limiting conditions enrich for fimbriate cells of uropathogenic *Proteus mirabilis* and *Escherichia coli*. *J Bacteriol* 191:1382–1392. <https://doi.org/10.1128/JB.01550-08>.
30. Struve C, Krogfelt KA. 1999. In vivo detection of *Escherichia coli* type 1 fimbrial expression and phase variation during experimental urinary tract infection. *Microbiology* 145:2683–2690. <https://doi.org/10.1099/00221287-145-10-2683>.

31. Gunther NW, Lockett V, Johnson DE, Mobley HLT. 2001. In vivo dynamics of type 1 fimbria regulation in uropathogenic *Escherichia coli* during experimental urinary tract infection. *Infect Immun* 69:2838–2846. <https://doi.org/10.1128/IAI.69.5.2838-2846.2001>.
32. Lim JK, Gunther NW, Zhao H, Johnson DE, Keay SK, Mobley HLT. 1998. In vivo phase variation of *Escherichia coli* type 1 fimbrial genes in women with urinary tract infection. *Infect Immun* 66:3303–3310.
33. Lloyd AL, Rasko DA, Mobley HL. 2007. Defining genomic islands and uropathogen-specific genes in uropathogenic *Escherichia coli*. *J Bacteriol* 189:3532–3546. <https://doi.org/10.1128/JB.01744-06>.
34. Subashchandrabose S, Hazen TH, Rasko DA, Mobley HL. 2013. Draft genome sequences of five recent human uropathogenic *Escherichia coli* isolates. *Pathog Dis* 69:66–70. <https://doi.org/10.1111/2049-632X.12059>.
35. Bielecki P, Muthukumarasamy U, Eckweiler D, Bielecka A, Pohl S, Schanz A, Niemeyer U, Oumeraci T, von Neuhoff N, Ghigo JM, Häussler S. 2014. In vivo mRNA profiling of uropathogenic *Escherichia coli* from diverse phylogroups reveals common and group-specific gene expression profiles. *mBio* 5:e01075-14. <https://doi.org/10.1128/mBio.01075-14>.
36. Korem T, Zeevi D, Suez J, Weinberger A, Avnit-Sagi T, Pompan-Lotan M, Matot E, Jona G, Harmelin A, Cohen N, Sirota-Madi A, Thaiss CA, Pevsner-Fischer M, Sorek R, Xavier RJ, Elinav E, Segal E. 2015. Growth dynamics of gut microbiota in health and disease inferred from single metagenomic samples. *Science* 349:1101–1106. <https://doi.org/10.1126/science.aac4812>.
37. Olm MR, Brown CT, Brooks B, Firek B, Baker R, Burstein D, Soenjoyo K, Thomas BC, Morowitz M, Banfield JF. 2017. Identical bacterial populations colonize premature infant gut, skin, and oral microbiomes and exhibit different in situ growth rates. *Genome Res* 27:601–612. <https://doi.org/10.1101/gr.213256.116>.
38. Brown CT, Olm MR, Thomas BC, Banfield JF. 2016. Measurement of bacterial replication rates in microbial communities. *Nat Biotechnol* 34:1256–1263. <https://doi.org/10.1038/nbt.3704>.
39. Mobley HL, Green DM, Trifillis AL, Johnson DE, Chippendale GR, Lockett CV, Jones BD, Warren JW. 1990. Pyelonephritogenic *Escherichia coli* and killing of cultured human renal proximal tubular epithelial cells: role of hemolysin in some strains. *Infect Immun* 58:1281–1289.
40. Mulvey MA, Schilling JD, Hultgren SJ. 2001. Establishment of a persistent *Escherichia coli* reservoir during the acute phase of a bladder infection. *Infect Immun* 69:4572–4579. <https://doi.org/10.1128/IAI.69.7.4572-4579.2001>.
41. Berger H, Hacker J, Juarez A, Hughes C, Goebel W. 1982. Cloning of the chromosomal determinants encoding hemolysin production and mannose-resistant hemagglutination in *Escherichia coli*. *J Bacteriol* 152:1241–1247.
42. Hooton TM, Scholes D, Stapleton AE, Roberts PL, Winter C, Gupta K, Samadpour M, Stamm WE. 2000. A prospective study of asymptomatic bacteriuria in sexually active young women. *N Engl J Med* 343:992–997. <https://doi.org/10.1056/NEJM200010053431402>.
43. Andersson P, Engberg I, Lidin-Janson G, Lincoln K, Hull R, Hull S, Svanborg C. 1991. Persistence of *Escherichia coli* bacteriuria is not determined by bacterial adherence. *Infect Immun* 59:2915–2921.
44. Hagberg L, Engberg I, Freter R, Lam J, Olling S, Svanborg Edén C. 1983. Ascending, unobstructed urinary tract infection in mice caused by pyelonephritogenic *Escherichia coli* of human origin. *Infect Immun* 40:273–283.
45. Johnson DE, Lockett CV, Russell RG, Hebel JR, Island MD, Stapleton A, Stamm WE, Warren JW. 1998. Comparison of *Escherichia coli* strains recovered from human cystitis and pyelonephritis infections in transurethrally challenged mice. *Infect Immun* 66:3059–3065.
46. Andrews S. FastQC. A quality control tool for high throughput sequence data. <http://www.bioinformatics.babraham.ac.uk/projects/fastqc/>.
47. Bolger AM, Lohse M, Usadel B. 2014. Trimmomatic: a flexible trimmer for Illumina sequence data. *Bioinformatics* 30:2114–2120. <https://doi.org/10.1093/bioinformatics/btu170>.
48. Langmead B, Salzberg SL. 2012. Fast gapped-read alignment with Bowtie 2. *Nat Methods* 9:357–359. <https://doi.org/10.1038/nmeth.1923>.